

REVIEW

The diagnosis, classification, and treatment of sarcoma in this era of artificial intelligence and immunotherapy

Amandine Cromb  ^{1,2} | Mathieu Rouleau-Dugage³ | Antoine Italiano^{4,2}

¹Department of Imaging, Institut Bergonié, Bordeaux, Nouvelle-Aquitaine F-33076, France

²Faculty of Medicine, University of Bordeaux, Bordeaux, Nouvelle-Aquitaine F-33000, France

³Department of Medicine, Gustave Roussy, Villejuif, Ile de France F-94800, France

⁴Early Phase Trials and Sarcoma Unit,
Institut Bergonié, Bordeaux,
Nouvelle-Aquitaine F-33076, France

Correspondence

Antoine Italiano, Early Phase Trials and Sarcoma Units, Institut Bergonié, 229 Cours de l'Argonne, Bordeaux, Nouvelle-Aquitaine F-33000, France.
Email: a.italiano@bordeaux.unicancer.fr

Funding information

Agence Nationale de la Recherche -
Recherche Hospitalo-Universitaire en
santé (RHU) CONDOR programme

Abstract

Soft-tissue sarcomas (STS) represent a group of rare and heterogeneous tumors associated with several challenges, including incorrect or late diagnosis, the lack of clinical expertise, and limited therapeutic options. Digital pathology and radiomics represent transformative technologies that appear promising for improving the accuracy of cancer diagnosis, characterization and monitoring. Herein, we review the potential role of the application of digital pathology and radiomics in managing patients with STS. We have particularly described the main results and the limits of the studies using radiomics to refine diagnosis or predict the outcome of patients with soft-tissue sarcomas. We also discussed the current limitation of implementing radiomics in routine settings. Standard management approaches for STS have not improved since the early 1970s. Immunotherapy has revolutionized cancer treatment; nonetheless, immuno-oncology agents have not yet been approved for patients with STS. However, several lines of evidence indicate that immunotherapy may represent an efficient therapeutic strategy for this group of diseases. Thus, we emphasized the remarkable potential of immunotherapy in sarcoma treatment by focusing on recent data regarding the immune landscape of these tumors. We have particularly emphasized the fact that the development of immunotherapy for sarcomas is not an aspect of histology (except for alveolar soft-part sarcoma) but rather that of the tumor microenvironment. Future studies investigating immunotherapy strategies in sarcomas should incorporate at least the presence of tertiary lymphoid structures as a stratification factor in their design, besides

List of abbreviations: ¹⁸F-FDG, ¹⁸F-fluoro-2-deoxyglucose; AI, artificial intelligence; BCR, B cell-related; c-index, concordance index; CE, contrast enhanced; CI, confidence interval; CINSARC, Complexity INdex in SARComas; CNN, convolutional neural network; CT, computed tomography; CTLA-4, cytotoxic T-Lymphocyte antigen 4; DWI, diffusion weighted imaging; FNCLCC, French ‘*Fédération National des Centres de Lutte Contre Le Cancer*’; FS, fat suppressed; IBSI, Imaging Biomarker Standardization Initiative ; ICIs, Immune checkpoint inhibitors; IHC, Immunohistochemistry; LAG3, lymphocyte activation gene-3; LFS, local relapse-free survival; MFS, metastatic relapse-free survival; MRCLPS, myxoid round cells liposarcoma; MRI, magnetic resonance imaging; OS, overall survival; PD-1, programmed cell death protein 1; PD-L1, programmed cell death ligand 1; PET, positron emission tomography; PERCIST, PET evaluation response criteria in solid tumor; PFS, progression free survival; RECIST, response evaluation criteria in solid tumors; PFS, progression free survival; RFs, radiomics features; RQS, radiomics quality score; RR, Response rate; STS, soft tissue sarcomas; TCR, T cell receptor; TILs, tumor infiltrating lymphocytes; TLS, tertiary lymphoid structure; TME, tumor microenvironment; WI, weighted imaging.

This is an open access article under the terms of the [Creative Commons Attribution-NonCommercial-NoDerivs](#) License, which permits use and distribution in any medium, provided the original work is properly cited, the use is non-commercial and no modifications or adaptations are made.

© 2022 The Authors. *Cancer Communications* published by John Wiley & Sons Australia, Ltd. on behalf of Sun Yat-sen University Cancer Center

including a strong translational program that will allow for a better understanding of the determinants involved in sensitivity and treatment resistance to immune-oncology agents.

KEY WORDS

artificial intelligence, digital pathology, immunotherapy, radiomics, sarcoma

1 | BACKGROUND

Soft-tissue sarcomas (STS) represent a heterogeneous group of tumors. An accurate histological diagnosis and an assessment of the risk of relapse are critical for delineating treatment strategies. Traditional pathology approaches and molecular genetic assays have played a crucial role in the classification of STS. Recently, artificial intelligence (AI)-based solutions paved the way for the development of digital pathology approaches, with whole-slide imaging that enables capturing relevant information beyond human visual perception. Such progress has been implemented in the field of imaging with the possibility of characterizing human tumors through “radiomics” analyses, which are based on several image-derived, quantitative measurements, including intensity histogram, spatial distribution relationships, and textural heterogeneity. Both digital pathology and radiomics approaches can be used to understand the relationships between histological and imaging characteristics of STS, such as heterogeneity and their biological characteristics or expected prognosis and treatment outcomes. Besides improving the staging and prognosis assessment, expanding the therapeutic armamentarium is another challenge for better care of patients with STS. Chemotherapy has reached a therapeutic plateau in this group of diseases [1]. Immunotherapy has revolutionized cancer treatment; nonetheless, immuno-oncology agents have not yet been approved for patients with STS. However, several lines of evidence suggest that immunotherapy may represent an efficient therapeutic strategy for this group of diseases.

In this review, we provide an up-to-date and state-of-the-art application of digital pathology and radiomics in managing patients with STS and the potential role of immunotherapy in improving patient outcomes.

2 | IMPROVING THE PROGNOSTICATION OF PATIENTS WITH STS THROUGH DIGITAL PATHOLOGY AND ARTIFICIAL INTELLIGENCE

Digital pathology is based on the use of algorithms, machine-learning techniques, and AI to extract infor-

mation from routine pathologic images. In recent years, several studies have demonstrated the potential of digital pathology in improving the diagnostic and staging workflow in human tumors. However, the application of digital pathology in STS is unclear.

STS constitutes a heterogeneous group of malignant tumors, representing 1% and 15% of cancer in adults and children, respectively [1]. Surgery is the cornerstone of treatment. However, up to 40% of the patients develop metastatic relapse despite optimal locoregional treatment, which leads to death in most cases [2]. Assessing the risk of relapse is an important concern for physicians managing these patients. Perioperative chemotherapy reduces the risk of relapse by approximately 30% [3–6]. However, identifying patients most likely to benefit from perioperative systemic treatment remains challenging [7]. Clinical factors, such as the grade, size, and depth of the tumors, are usually associated with the risk of metastatic relapse and are considered by oncologists for assessing the relapse risk [8]. A nomogram may serve as a convenient and reliable tool for the individualized prediction of recurrence [2, 9]. However, this method is not perfect. Combining gene expression profiling data through the Complexity INdex in SARComas (CINSARC) signature improves the nomogram, thereby enhancing the prediction of relapse [10]. Moreover, despite the increasing incorporation of genomic profiling into patient care, the procedure is not routinely followed at most healthcare facilities handling sarcoma cases.

Recently, AI has appeared promising in predicting the prognosis of several conditions [11]. There are reports on the emergence of models that could directly predict disease outcomes from digitized whole-slide images of mesothelioma [12] or hepatocellular carcinoma [13] using deep-learning methods. These models outperformed the previous methods that relied on expensive and time-consuming expert annotations or gradings for producing results. In addition, multiple studies have demonstrated the benefits of performing a multimodal analysis to complement AI image analysis with expert knowledge and clinical data [14]. Foersch et al. [15] reported an example of such synergy for STS by predicting the disease-specific survival in specific STS subtypes. They demonstrated the ability of multimodal machine

learning to predict metastatic relapse in patients with STS.

Taken together, researchers are initiating the deployment of digital pathology. Such machine learning-based digital models may be potentially transformative for managing patients in a routine setting.

3 | INNOVATIVE IMAGING TECHNIQUES TO IMPROVE THE MANAGEMENT OF PATIENTS WITH SARCOMA

Besides an accurate histological diagnosis, imaging is fundamental to every step involved in managing patients with STS, including the initial referral to a sarcoma reference center, biopsy guidance, local and distant tumor staging, surgery planning, follow-up, and response assessment [16]. Imaging provides a non-invasive and global view of the tumor phenotype (or radiophenotype) that complements biopsy sample-based assays. The commonly used prognostic nomogram SARCULATOR [9] and response evaluation criteria for STS (response evaluation criteria in solid tumors [RECIST v1.1]) [17] rely only on the simplest imaging feature, namely the longest tumor diameter, despite STS demonstrating various baseline radiological presentations and patterns of response under treatment.

However, the last few decades have witnessed the following development: (i) radiomics-based approaches, (ii) quantitative multi-parametric imaging enabling the non-invasive assessment of tumor neo-angiogenesis (through dynamic contrast-enhanced [CE] magnetic resonance imaging [MRI]), cell shape and density (through diffusion-weighted imaging [DWI]), and metabolism (through ^{18}F -fluoro-2-deoxyglucose [^{18}F -FDG] positron emission tomography [PET] computed tomography [CT]), and (iii) novel radiolabeled antibodies in preclinical studies and phase I/II clinical trials [18–22]. The parallel innovation and increasing availability of AI algorithms for the classification, prognostication, clustering, and computer vision tasks have enabled capturing and integration complex datasets to achieve a virtual diagnosis and improve the prognostication and treatment response assessment.

3.1 | Principle of radiomics approaches

The radiomics technique involves the extensive quantification of the tumor shape and texture based on any imaging modality beyond the conventional radiologist's depiction, using mathematical operators, such as histograms, gray level matrices, and wavelet or fractal analyses (Figure 1). Subsequently, hundreds of resulting numeric variables,

termed radiomics features (RFs), are incorporated and mined using machine-learning algorithms to develop predictive models aimed at improved tailoring of patient management [20, 23]. Radiomics approaches rely on complex pipelines, including the selection and quality control of imaging, homogenization of an imaging dataset to ensure comparability, manual or semi-automatic segmentation of the volume of interest (for instance, the primitive tumor itself, its surrounding tissues, or metastases), RF extraction, exploratory data analysis, the use of techniques to correct for imbalanced datasets, dimensionality reduction, training multiple machine-learning algorithms using resampling methods (such as nested cross-validation), and testing on novel original datasets to evaluate and select the best model objectively. This empirical process implies defining a metric for measuring the performance of the trained machine-learning models depending on the final objective of the radiomics study and the distribution of the outcomes in the study population. For instance, the area under the receiver operating characteristic curve (AUC) and accuracy, Harrell concordance index (c-index) and root mean squared error are commonly encountered for binary classification, prognostication and regression problems, respectively [24]. Calibration curves and decision curve analysis are additional means to evaluate the radiomics models [20, 25]. Due to this complexity, radiomics approaches are qualified as “handcraft.” Recently, researchers have developed alternative RFs, termed deep-learning RFs, using transfer learning, namely convolutional neural networks (CNNs) previously trained on the Imagenet dataset, such as Xception [26], VGG16 [27] and 19 [28], ResNet50 [29], or InceptionResNetV2 [30]. These deep-learning RFs supposedly provide higher reproducibility than handcraft RFs [31]. Moreover, radiomics composite scores are often integrated into nomograms along with the clinical, biological, and histopathological features, which generally improve their predictive performances [32–37].

3.2 | Applications of radiomics approaches for patients with STS

Since its emergence in the early 2010s, clinicians have commonly used radiomics in the field of STS. STS exhibits various radiological presentations with different patterns of heterogeneity that are barely explainable using human vocabulary and usual radiological qualitative or semi-quantitative variables (also termed “semantic” features). Nonetheless, a key assumption behind radiomics is that these heterogeneity patterns reflect different subtypes of STS in terms of molecular features, treatment sensitivity, and prognosis [38].

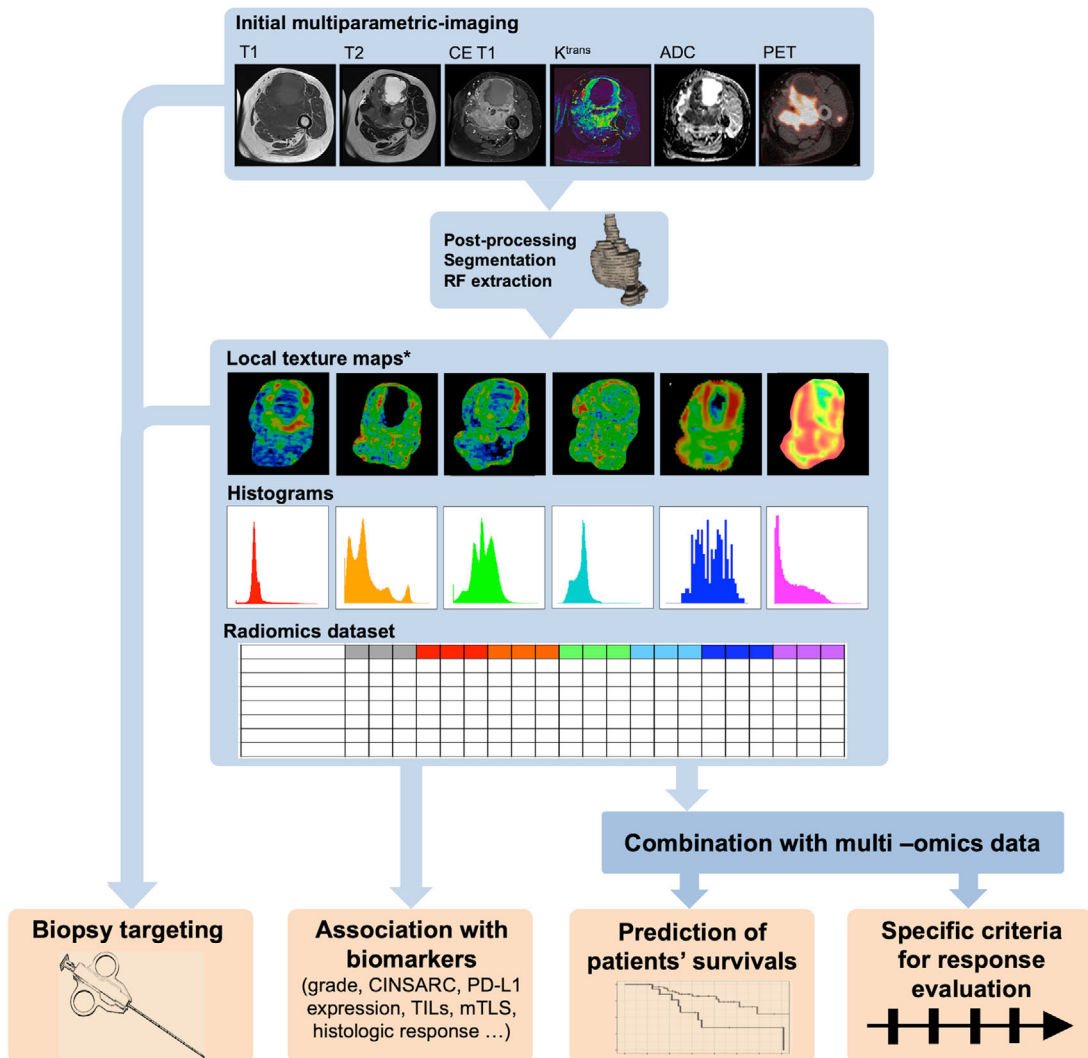


FIGURE 1 The radiomics workflow and potentialities adapted to baseline multi-parametric multimodal imaging of a patient with soft-tissue sarcoma. A schematic illustration of the patient's journey, including image acquisition, analysis utilizing radiomics, and other clinical and biological variables to derive a predictive signature of the patient's outcome. High-level statistical modeling involving machine learning is applied for disease classification, patient clustering, and individual risk stratification. Abbreviations: ADC: apparent diffusion coefficient, CE T1: contrast-enhanced T1, CINSARC: complexity index in sarcoma signature, K^{trans}: transfer constant, mTLS: mature tertiary lymphoid structure, PD-L1: program death ligand 1, PET: (18F-fluorodeoxyglucose) positron emission tomography, RF: radiomics features, and TILs: tumor infiltrative lymphocytes.

Tables 1 and 2 summarize the major published sarcoma radiomics studies using CT and MRI. First, MRI-based radiomics from conventional sequences (T1-weighted imaging [WI], T2-WI, and CE T1-WI) and DWI have demonstrated high diagnostic performance in discriminating between benign soft-tissue tumors and STS (accuracy: 0.65–0.93 and AUC: 0.77–0.97 for approximately 609 unique patients) [32, 39–42]. Some authors have obtained good results for the peculiar but routine issues of discriminating lipoma from liposarcomas (AUC: 0.8–0.98 and accuracy: 0.87–0.95) [43–48] and leiomyoma from uterine sarcoma (AUC: 0.83–0.96 and accuracy: 0.74–0.88) [49–53]. Second, radiomics approaches have successfully predicted

the histologic grade (according to the French “*Fédération Nationale des Centres de Lutte Contre le Cancer*”) from pre-treatment MRIs (AUC: 0.76–0.92, accuracy: 0.82–0.98 for approximately 1,080 unique patients) [31, 33–35, 54, 55]. However, these authors used different definitions of high grade (i.e., grade II and III versus only grade III), and the grade was occasionally evaluated on biopsy samples, despite the possibility of grade underestimation and biased results [56, 57].

Clinicians have applied radiomics to predict patient prognosis, predominantly metastatic relapse-free survival (MFS), local relapse-free survival (LFS), overall survival (OS), and the risk of presenting lung metastases

TABLE 1 Summary of the main radiomics studies involving the initial diagnosis and staging of sarcoma

First author	Year	Question	No. of patients	Imaging modality	Results	Main limitations
Uterine leiomyosarcoma versus leiomyoma						
Gerges et al. [49]	2018	Discrimination of leiomyomas versus leiomyosarcomas	68 patients from 1 cohort (17 leiomyosarcomas)	MRI (T1, T2, ADC)	Two independent predictors (age and mean T2 signal); AUC = 0.955§.	Retrospective; no image post-processing for heterogeneous datasets; no reproducibility analysis; only one algorithm tested; no validation cohort; no comparisons with radiologists; no available code.
Nakagawa et al. [50]	2019	Discrimination of leiomyomas versus leiomyosarcomas with high signal intensities on T2.	80 patients from 1 center (30 leiomyosarcomas)	MRI (T2)	Model using extreme gradient boosting; AUC = 0.95§; outperformed radiologists' prediction.	Retrospective; no image post-processing for heterogeneous datasets; 2D ROIs; no reproducibility analysis; no validation cohort; no available code.
Xie et al. [51]	2019	Discrimination of uterine sarcoma and atypical leiomyoma	78 patients from 1 center (29 leiomyosarcomas)	MRI (ADC)	Model using logistic regression; AUC = 0.830, accuracy = 0.74, Se = 0.76, Sp = 0.73§.	Retrospective; no image post-processing for heterogeneous datasets; no reproducibility analysis; only one algorithm tested; no validation cohort; no available code.
Wang et al. [52]	2021	Discrimination of leiomyomas and malignant uterine mesenchymal tumors	134 patients from 1 center (30 malignant tumors) divided into training and testing sets	MRI (T2)	Model using SVM and LASSO; AUC = 0.76; best performance obtained with a mixed model clinical-radiomics model (AUC = 0.91), similar to senior radiologist (AUC = 0.90)	Retrospective; only one algorithm tested; no available code.
Dai et al. [53]	2022	Discrimination of uterine sarcoma and atypical leiomyoma	172 patients from 1 center (86 malignant tumors) divided into training and testing sets	MRI (T2, ADC)	Model using Random Forests on clinical data and deep-learning features; AUC = 0.96, accuracy = 0.88; outperformed models on deep-learning features alone, handcrafted radiomics features (\pm clinical data)	Retrospective; only one algorithm tested; no comparisons with radiologists; no available code

(Continues)

TABLE 1 (Continued)

First author	Year	Question	No. of patients	Imaging modality	Results	Main limitations
Lipoma vs liposarcoma						
Thornhill et al. [43]	2014	Discrimination of lipoma and LPS	44 patients from 1 center (20 LSSs)	MRI (T1)	Model using linear discriminant analysis; $AUC = 0.98$, $Se = 0.95$, $Sp = 0.87\delta$; outperformed radiologists' predictions.	Inclusion of myxoid and de-differentiated LPS; retrospective; no reproducibility analysis; no validation cohort; no available code
Vos et al. [44]	2019	Discrimination of lipoma and well-differentiated LPS or ALT	116 patients from 1 center (58 ALTs)	MRI (T1, T2)	Models combining multiple ML algorithms; $AUC = 0.89$, $Se = 0.74$, $Sp = 0.88\delta$; outperformed radiologists' prediction	Retrospective; no image post-processing for heterogeneous datasets; no reproducibility analysis; no validation cohort; no available code
Pressney et al. [45]	2020	Discrimination of lipoma and well-differentiated LPS or ALT	60 patients from 1 center (30 ALTs)	MRI (PD, T1)	Score combining texture and radiological features; $AUC = 0.8$, $Se = 0.9$, $Sp = 0.6\delta$	Retrospective; no image post-processing for heterogeneous datasets; no reproducibility analysis; no machine-learning algorithm; no resampling; no validation cohort; no comparison with radiologists; no available code
Malinauskaitė et al. [46]	2020	Discrimination of lipoma and LPS	38 patients from 1 center (14 LSSs)	MRI (T1)	Model using SVM; $AUC = 0.926$, accuracy = 0.95, $Se = 0.89$, $Sp = 1\delta$; outperformed radiologists' prediction	Inclusion of myxoid and de-differentiated LPS; retrospective; no image post-processing for heterogeneous datasets; no validation cohort; no available code.
Lepotrig et al. [47]	2020	Discrimination of lipoma and well-differentiated LPS or ALT	81 patients from 1 center (40 ALTs)	MRI (fat-suppressed CE-T1)	Model using SVM; $AUC = 0.96$, accuracy = 0.95, $Se = 1$, $Sp = 0.9\delta$	Retrospective; no image post-processing for heterogeneous datasets; no validation cohort; no comparison with radiologists; no available code.

(Continues)

TABLE 1 (Continued)

First author	Year	Question	No. Of patients	Imaging modality	Results	Main limitations
Yang et al. [48]	2022	Discrimination of lipoma and well-differentiated LPS or ALT using deep-learning-feature or handcrafted radiomics analysis	127 patients from 2 centers (58 ALTs) divided into training and testing sets	CT-scan and MRI (T1, T2)	Nomogramm using clinical, biological and deep-learning signature; AUC = 0.94, accuracy = 0.87, Se = 0.95, Sp = 0.78; outperformed radiomics and radiologists.	Retrospective; no image post-processing for heterogeneous dataset; no synthetic/adversarial data; no available code.
Benign soft tissue tumors versus soft-tissue sarcoma						
Juntu et al. [39]	2010	Discrimination between benign and malignant STTs	135 patients from 1 center (49 malignant tumors)	MRI (T1)	Model using SVM; AUC = 0.02, accuracy = 0.93, Se = 0.94, Sp = 0.91§; outperformed radiologists.	Retrospective; no image post-processing for heterogeneous datasets; 2D square ROIs instead of ED VOIs; no reproducibility analysis; no validation cohort; no available code.
Martin-Carreras et al. [40]	2019	Discrimination between myxoma and myxofibrosarcoma	56 patients from 1 center (27 myxofibrosarcomas)	MRI (T1)	Model using random forests, AUC = 0.88, accuracy = 0.84, Se = 0.85, Sp = 0.83§.	Retrospective; T1 sequence not appropriate for myxoid tumor; no reproducibility analysis; no validation cohort; no comparison with radiologists; no available code.
Fields et al. [41]	2021	Discrimination between benign and malignant STTs	128 patients from 1 center (92 malignant tumors)	MRI (T1, CE-T1, T2, PD ± fat suppression)	Model using AdaBoost on multiple sequences; AUC = 0.77, Se = 0.87, Sp = 0.34§; simpler model using random forests on fat suppressed T2 (AUC = 0.75§)	Retrospective; no image post-processing for heterogeneous datasets; no reproducibility analysis; no validation cohort; no comparison with radiologists; no available code.
Lee et al. [42]	2021	Discrimination between benign and malignant STTs	151 patients from 1 center (71 malignant tumors) divided into training and testing sets	MRI (ADC)	Model using random forest on radiomics, ADCminimal and ADCmean; AUC = 0.77-0.81, accuracy = 0.65-0.71, Se = 0.71-0.83, Sp = 0.59	Retrospective; no available code.

(Continues)

TABLE 1 (Continued)

First author	Year	Question	No. of patients	Imaging modality	Results	Main limitations
Yue et al. [32]	2022	Discrimination between benign and malignant STTs	139 patients from 1 center (75 malignant tumors) divided into 3 cohorts	MRI (T2 with fat suppression, CE T1)	Nomogram model using radiomics scores build with LASSO logistic regression and clinical-radiological variables; AUC = 0.95, accuracy = 0.87, Se = 0.81, Sp = 0.95	Retrospective; no image post-processing for heterogeneous datasets; no reproducibility analysis; no comparison with radiologists; no available code.
Corino et al. [34]	2018	Grading of STS using radiomics	19 patients from 1 center (14 with grade 3 STS)	MRI (ADC)	Model using histogram-based features; $AUC = 0.87$, $accuracy = 0.98\%$	Retrospective; very small and heterogeneous dataset; no image post-processing for heterogeneous datasets; no reproducibility analysis; only one tested algorithm; no validation cohort; no comparison with radiologists; no available code.
Peeken et al. [33]	2019	Grading of STS using radiomics	225 patients from 2 centers (157 patients with grade 2/3 STS) divided into training and testing sets	MRI (fat-suppressed T2 and CE-T1)	Model using penalized logistic regression; $AUC = 0.76$, accuracy = 0.83, Se = 0.9, Sp = 0.5; outperforms clinical model. Nomogram using T2 radiomics score and TNM staging better predicts OS than stage alone (c-indices = 0.74 versus 0.69).	Retrospective; grade assessed on biopsy at risk of underestimation; splits depending on center at risk of center bias; no comparison with radiologists; no available code.
Zhang et al. [35]	2019	Grading of STS using radiomics	35 patients from 1 center (26 with grade 2-3 STS)	MRI (fat-suppressed T2)	Model using SVM; $AUC = 0.92$, accuracy = 0.88, Se = 0.92, Sp = 0.89%.	Retrospective; no image post-processing for heterogeneous datasets; no reproducibility analysis; no validation cohort; no comparison with radiologists; no available code.

(Continues)

TABLE 1 (Continued)

First author	Year	Question	No. Of patients	Imaging modality	Results	Main limitations
Yan et al. [34]	2021	Grading of STS using radiomics	180 patients from 2 centers (87 with grade 3 STS) divided into training and testing sets	MRI (T1, fat-suppressed T2)	Nomogram including radiomics score using LASSO logistic regression; AUC = 0.88, accuracy = 0.82, Se = 0.84, Sp = 0.79; outperformed clinical-radiological model; moderate performances for PFS prediction (c-index = 0.58)	Retrospective; splits depending on center at risk of center bias; only one tested algorithm; no available code
Navarro et al. [31]	2021	Improvement in grade classification performances using deep-learning features instead of handcrafted radiomics features	306 patients from 2 centers (229 patients with grade 2-3 STS) divided into training and testing sets	MRI (fat-suppressed T2 and CE-T1)	Model using deep learning on fat suppressed T2; AUC = 0.76, accuracy = 0.83, Se = 0.91, Sp = 0.40; similar as radiomics but more reproducible	Retrospective; grade assessed on biopsy at risk of underestimation; deep-learning features assessed on a single 2D slice at risk of sampling bias; splits depending on center at risk of center bias; no synthetic data for deep learning; no comparison with radiologists; no available code
Yang et al. [35]	2022	Improvement in grade classification performances using deep-learning features instead of handcrafted radiomics features	540 patients from 1 center (309 with grade 2-3 STS) divided into training and testing sets	MRI (T1, fat-suppressed T2)	Nomogram including deep-learning signature (ResNet50) using support vector machines; AUC = 0.87, accuracy = 0.83, Se = 0.85, Sp = 0.78; outperformed clinical and handcrafted radiomics models; correlated with overall survival	Retrospective; no synthetic data for deep learning; unclear management of 3D tumor volume in deep-learning analysis; no comparison with radiologists; no available code

NOTE.- Abbreviations: ADC: apparent diffusion coefficient, ALT: atypical lipomatous tumor, AUC: area under the ROC curve, CE: contrast-enhanced, LASSO: least absolute shrinkage and selection operator, IPS: liposarcoma, ML: machine learning, MRI: magnetic resonance imaging; PD: proton density, PFS: progression-free survival; Se: sensitivity, Sp: specificity, STS: soft tissue sarcoma, SVM: support vector machine. §: the text in italic corresponds to performances that were only evaluated on the training cohort and not on an independent test set, and thus, likely to be overestimated. Of note, only studies with multivariate analyses and CT-scan or MRI are presented. For multiple publications from the same cohorts, we only present the largest and more impactful one.

TABLE 2 Summary of the main radiomics studies involving the prognostication and the prediction of response to neoadjuvant treatment in sarcoma patients

First author	Year	Question	No. Of patients	Imaging modality	Results	Main limitations
Vallières et al. [58]	2015	Prediction of lung metastatic relapse in STS patients. Methods to optimize fusion of PET and MR imaging. Influence of processing on predictions.	51 patients from the TCIA dataset	PET-CT and MRI (T1, fat-suppressed T2)	Model using logistic regression; $AUC = 0.98$, $Se = 0.96$, $Sp = 0.93\delta$.	Retrospective; only one algorithm tested; no comparison with radiologists; no validation cohort
Peeken et al. [59]	2019	Prognostication of STS using radiomics (LFS, MFS, OS).	212 patients from 3 centers, divided into 1 training and 2 testing sets	CT-scans	Models using gradient boosting to predict LFS (c-index = 0.77), MFS (c-index = 0.68-0.73) and OS (c-index = 0.59-0.73); also models using random forests to predict grading ($AUC = 0.64$). Radionics models outperformed clinical models for LFS.	Retrospective; use of CE and non-CE CT-scans; splits depending on center at risk of bias; only one algorithm tested; no comparison with radiologists; no available code
Crombé et al. [60]	2020	Prediction of metastatic relapse at 2 years in patients treated with NAC; the influence of signal intensity harmonization methods on prediction.	70 patients from 1 center divided into training and testing sets	MRI (T2)	Model using elasticnet logistic regression; $AUC = 0.82$, accuracy = 0.75; best performances reached with histogram matching method.	Retrospective; only one tested algorithm; no comparison with radiologists; no available code
Crombé et al. [61]	2020	Prediction of MFS in myxoid/round cells liposarcomas	35 patients from 1 center	MRI (T2)	Model using LASSO Cox regression on radiological and radionics features; c-index = 0.93\delta	Retrospective; heterogeneous patient management (\pm NAC); small dataset; only one algorithm tested; no validation cohort; no available code
Crombé et al. [65]	2020	Prediction of MFS in STS patients treated with NAC. Development of methods to quantify the intra-tumoral heterogeneity in neo-angiogenesis.	50 patients from 1 center	MRI (T2, DCE-MRI)	Best model using LASSO Cox regression and combination of radiological and radionics features from T2 + DCE-MRI; c-index = 0.84\\$. Better performance with radionics directly extracted from raw DCE-MRI data than from parametric maps.	Retrospective; only one algorithm tested, no validation cohort; no available code

(Continues)

TABLE 2 (Continued)

First author	Year	Question	No. Of patients	Imaging modality	Results	Main limitations
Yang et al. [62]	2021	Prediction of OS using radiomics after curative treatment.	353 patients from 1 center, divided into training and testing sets.	CT-scan	Models using random survival forests and radiomics, age, lymph node involvement, and FNCLCC grade, c-index ≈ 0.80.	Retrospective; unknown contrast agent injection; no image post-processing for heterogeneous datasets; no reproducibility analysis; no comparisons with radiologists and between models; no available code
Peeken et al. [63]	2021	Prediction of OS using radiomics. Comparison with conventional radiological analysis.	179 patients from 2 centers, divided into training and testing sets	MRI (T1, fat-suppressed T2)	Model using radiomics from T2, AJCC and age; c-index = 0.73; outperformed other combinations of clinical, radiologic and radiomics features.	Retrospective; heterogeneous patients' management (\pm NART); splits depending on center at risk of center bias; no available code
Chen et al. [36]	2021	Prognostication of STS treated with NART using radiomics (MFS)	62 patients from 1 center and TCIA	MRI (fat suppressed T2)	Nomogram using radiomics score (built with LASSO Cox regression), tumor size and location; c-index = 0.78%; outperformed clinical stage and radiomics score alone.	Retrospective; no image post-processing for heterogeneous datasets; only one tested algorithm; no validation cohort; no comparison with radiologists; no available code
Faddi et al. [64]	2022	Prognostication of STS using delta-radiomics clusters assessing natural tumor evolution (LFS, MFS, OS)	68 patients from 1 center	MRI (CE-T1)	Unsupervised classification based on logarithmic changes in radiomics features before treatment beginning is an independent predictor of LFS, but not MFS or OS.	Retrospective; only one tested algorithm; no validation cohort
Liu et al. [37]	2022	Prediction of LFS using deep-learning radiomics. Comparisons with handcraft radiomics features.	282 patients from 3 centers, divided into training and testing sets	MRI (T1, T2, ± CE-T1)	Nomogram using deep-learning radiomics score, NCI, histology, Ki67 (c-index = 0.77). Outperforms usual staging systems, but the best performance was reached by Ki67 alone (c-index = 0.76).	Retrospective; unclear management of ROIs (2D or 3D?) and multiple sequences; splits depending on center at risk of center bias; no synthetic data for deep learning; only one algorithm tested; no comparison with radiologists; no available code

(Continues)

TABLE 2 (Continued)

First author	Year	Question	No. Of patients	Imaging modality	Results	Main limitations
Prediction of response to treatment						
Crombé et al. [66]	2019	Prediction of histologic response (<10% viable cells on surgical specimen) following NAC in high-grade STS using delta-radiomics.	65 patients from 1 center (16 good responders), divided into training and testing sets	MRI (T2) at baseline and after 2 out of 6 cycles	Model using random forests on radiomics and radiological features; AUC = 0.63, accuracy = 0.75, Se = 0.98, Sp = 0.28; outperforms RECIST v1.1. Systematic errors to predict response in STS with abundant necrosis and bleeding.	Retrospective; lack of consensus on the definition of histologic response; no comparison with Choi criteria; no available code.
Crombé et al. [67]	2019	Prediction of histologic response (<10% viable cells on surgical specimen) following NAC in high-grade STS using radiomics from DCE-MRI. Influence of temporal parameters of DCE-MRI sequence on response prediction	25 patients from 1 center (5 good responders), prospective cohort.	MRI (DCE-MRI) at baseline	Model using logistic regression on radiomics; AUC = 0.90§. Best performance with sequence lasting 5 min at a temporal resolution of 6 sec.	Small dataset; lack of consensus on the definition of histologic response; only one tested algorithm; no validation cohort; no comparison with radiologists; no available code.
Gao et al. [68]	2020	Prediction of histologic response (<50% viable cells on surgical specimen) using radiomics (at baseline, after 3rd fraction and after NART) and delta-radiomics	30 patients from 1 center (unclear no. of good responders)	MRI (ADC)	Model using SVM and radiomics and delta-radiomics assessed at the 3 time points; AUC = 0.91, accuracy = 0.92, Se = 0.90, Sp = 0.97§.	Retrospective; lack of consensus on the definition of histologic response; no validation cohort; no comparison with Choi criteria and radiologists; no available code.
Peeken et al. [69]	2021	Prediction of histologic response (<5% viable cells on surgical specimen) using radiomics (before and after NART) and delta-radiomics	156 patients from 2 centers (16 good responders), divided into training and testing sets.	MRI (fat suppressed T2, CE-T1)	Model using random forests on radiomics and delta-radiomics; AUC = 0.75. Delta radiomics improve prediction compared to single timepoint radiomics alone.	Retrospective; heterogeneous patient management (\pm NAC); lack of consensus on the definition of histologic response; no validation cohort; no comparison with RECIST, Choi criteria, or radiologists

Abbreviations: ADC: apparent diffusion coefficient, AUC: area under the ROC curve, c-index: Harrell concordance index, CE: contrast-enhanced, DCE-MRI: dynamic contrast-enhanced MRI, LASSO: least absolute shrinkage and selection operator, LFS: local relapse-free survival, MFS: metastatic relapse-free survival, ML: machine learning, MRI: magnetic resonance imaging, NAC: neoadjuvant chemotherapy, NART: neoadjuvant radiotherapy, OS: overall survival, PD: proton density, PFS: progression-free survival, Se: sensitivity, Sp: specificity, STS: soft tissue sarcoma, SVM: support vector machine. §: the text in italic corresponds to performances that were only evaluated on the training cohort and not on an independent test set, and thus, likely to be overestimated. Of note, only studies with multivariate analyses and CT-scan or MRI are presented. For multiple publications from the same cohorts, we only present the largest and more impactful one.

following initial treatments (either curative surgery alone or neoadjuvant radiotherapy/chemotherapy followed by curative surgery). The resulting radiomics prognostic models demonstrated good to strong performances (c-index: 0.77 for LFS, 0.84–0.93 for MFS, and 0.73–0.80 for OS) [36, 58–65]. Eventually, radiomics has demonstrated the ability to predict the histologic response following neoadjuvant treatments using baseline RFs and delta-radiomics, which correspond to a quantitative change in RFs between two radiological evaluations. Despite variations in the definitions for the histological response across studies (<5%, <10%, and <50% of the viable tumor cells on surgical samples), all studies demonstrated significant associations between the radiomics models and response (AUC: 0.63–0.91 and accuracy: 0.75–0.92) [66–69]. The major secondary findings were as follows: (i) radiomics approaches appeared to provide better predictions than conventional tools (RECIST v1.1 and semantic radiological analysis alone), (ii) delta-radiomics improved performances compared with single timepoint radiomics, and (iii) models directly designed to predict prognosis were more effective than those initially designed to predict the grade [33, 66, 68, 69].

These encouraging results support the need to better incorporate quantitative information from medical imaging because the radiophenotype of STS is related to each clinically relevant outcome. However, no study has investigated the association between any imaging biomarker (including radiomics) and the gene expression profiles in STS (including the CINSARC signature) or their potential synergy with the circulating tumor DNA [70]. Eventually, combining multimodal multi-parametric imaging and AI could enable performing a “virtual biopsy,” i.e., a comprehensive and non-invasive assessment of the tumor’s pathological, molecular and prognostic features in cases where an actual biopsy is rarely feasible or insufficiently contributive.

3.3 | Current limitations to the clinical applications of radiomics and the means to overcome them

Researchers have to address several obstacles common to imaging biomarkers [71], namely biological correlations, reproducibility and repeatability of the radiomics model, feasibility in other centers, external validation, comparisons against the reference methods with a distinct added value, and prospective validation in decision-making situations. Thus, no radiomics signature is currently in routine clinical use regardless of the cancer type.

However, implementing radiomics in the routine setting has several limitations, which the radiomics community is

aware of and has endorsed several proposals to overcome. First, they have created an international collaboration, termed the Imaging Biomarker Standardization Initiative (IB, to standardize the methodology behind radiomics and the definitions of RFs, and provide several recommendations to perform distinct radiomics studies (<https://ibsi.readthedocs.io/en/latest/>) [72, 73]. Second, Lambin et al. [20] have proposed a score, termed the radiomics quality score (RQS), to quantify the quality of any radiomics study. The RQS consists of 16 items covering each study step, which can be used as support while designing a radiomics signature. Third, sharing databases with well-labeled imaging datasets and open-source codes to test the radiomics signatures would undeniably increase the confidence in radiomics and fill the translational gaps. The cancer imaging archive is the most famous of the initiatives to host freely available imaging datasets (<https://www.cancerimagingarchive.net/>) [74]. A small sarcoma dataset with PET-CT and conventional MRI is already present and included in radiomics studies; however, greater efforts are needed.

Moreover, the tedious and time-consuming manual segmentations of the tumor volume and the lack of practical and user-friendly applications for clinicians impose restrictions on radiomics. (Semi) automated segmentations using a deep-learning U-net CNN are expected to facilitate the segmentation step in the future [75]. Eventually, fully-automated pipelines that rely on deep-learning algorithms directly applied to the raw 3-D images should be able to capture the information better, owing to numerous and more personalized features for sarcoma.

4 | IMPROVING THE TREATMENT OF PATIENTS WITH STS THROUGH IMMUNOTHERAPY OF SARCOMAS

STS presents a unique treatment challenge because of the lack of improvement in the existing standard of care (such as doxorubicin) since the early 1970s [76]. Immune checkpoint inhibitors (ICIs) have been approved for more than 15 cancer indications; however, this is not the case for sarcomas [77]. Several biological aspects of STS suggest a strong rationale for immunotherapy as follows: (i) the presence of chromosomal translocations that result in unique fusion proteins, (ii) the high expression of tumor-associated antigens, of which the group of cancer-testis antigens, such as NY-ESO-1, are expressed by 80% of synovial sarcomas [78] and 90% of myxoid liposarcomas [79, 80], and partially (iii) the moderate frequency of genetic mutations (e.g., PIK3CA in 18% of myxoid liposarcomas, TP53 in 17% of pleomorphic liposarcomas, and NF1 in 11% of myxofibrosarcomas and 8% of pleomorphic liposarcomas). These aspects may

represent foreign antigens that can be targeted either by the natural immune response or actively induced immune response through immunotherapy.

Naturally-occurring immune infiltrates have been reported in several STS subtypes. Orui et al. [81] detailedly characterized the immune infiltrates in numerous STS subtypes with the detection of cytotoxic CD8+ T cells expressing granzyme B, thus indicative of their cytotoxic function; the dendritic cells were CD1a-negative but CD83-positive, thus indicating a mature phenotype. Furthermore, Tseng et al. [82] suggested an adaptive immune response with the presence of intratumoral lymphoid structures. In liposarcomas, CD8+ T cells appeared scattered throughout the tumor, whereas CD4+ T cells and CD20+ B cells were localized to these lymphoid structures. The presence of immune infiltrates in STS suggests the feasibility of immunotherapy for these subtypes.

4.1 | Role of ICIs in patients with STS

Despite the recent success of ICIs, there are limited and controversial human data to support the efficacy of immunotherapy in STS across immunotherapy clinical trials conducted in patients with STS [83].

A non-comparative randomized phase II study conducted on 85 patients with refractory STS compared the treatment with nivolumab versus nivolumab + ipilimumab, revealing a 5% response rate (RR) with nivolumab alone, whereas the combination displayed promising antitumor activity with a 16% RR [84]. Another phase II study, SARC028, demonstrated an RR of 40% for undifferentiated pleomorphic sarcoma and 20% for de-differentiated liposarcoma under pembrolizumab treatment [85]. In contrast, a phase II study conducted by the French Sarcoma Group demonstrated only one response among 50 evaluated STS patients treated with pembrolizumab plus oral cyclophosphamide [86].

We recently reported a pooled analysis of clinical trials investigating the efficacy of ICIs on sarcomas [87]. This study included 384 patients from nine clinical trials; of these patients, 153 (39.8%) received a programmed cell death protein 1 (PD-1) or programmed cell death-ligand 1 (PD-L1) antagonist as a single agent. The overall objective response rate (ORR) was 15.1% (95% confidence interval [CI]: 8.6%–25.1%). However, it dropped to 9.8% upon excluding alveolar soft-part sarcoma, an extremely rare sarcoma subtype displaying exquisite sensitivity to PD-1/PD-L1 monoclonal antibodies, from the analysis [88, 89].

Overall, all studies investigating ICIs included patients without applying any biomarker-based selection strategy (Table 3). Researchers have observed anecdotal responses in some histological subtypes (e.g., undifferentiated pleo-

morphic sarcomas or de-differentiated liposarcomas), which might be more sensitive to treatment [84, 85]. PD-L1 expression, currently used as a biomarker for immunotherapy in several epithelial tumors (non-small cell lung cancer, head and neck, and triple-negative breast cancer), is not relevant for STS. An overall PD-L1 expression of $\geq 1\%$ in tumor cells was observed in $> 15\%$ of the patients, without distinct correlation with the clinical benefits [87]. Moreover, the tumor mutation burden was low, with a median burden of fewer than two mutations/Mb across all histological subtypes [90].

For an in-depth investigation of the therapeutic impact of ICIs in patients with sarcoma and its correlation with the sarcoma microenvironment, we conducted an extensive analysis of the immune landscape of sarcomas [91]. By analyzing transcriptomic data from more than 600 STSs, we identified a subgroup of sarcomas classified as “immune high,” characterized by an elevated expression of a B cell-related (BCR) gene signature, which was predictive of survival, independent of the level of CD8+ T cell infiltration [91]. In addition, an immunohistochemistry (IHC) analysis revealed that this class of sarcoma is characterized by the presence of intratumoral tertiary lymphoid structures (TLSs) [91]. TLSs are ectopically formed aggregates of B-cell follicles, follicular dendritic cells, and CD4+ and CD8+ T cells, which play a critical role in anti-cancer immunity in several tumor types [92]. Moreover, a retrospective analysis of the biopsies from 47 patients included in the SARC028 study indicated that the BCR gene signature was highly predictive of the response to the anti-PD-1 antibody pembrolizumab, thereby suggesting that the presence of TLSs may serve as a robust biomarker for immunotherapy customization in patients with sarcoma [91].

Subsequently, we amended the PEMBROSARC study (NCT02406781; sponsor: Institut Bergonié, Bordeaux, France) to include a recent cohort, which was based on the presence of TLSs to investigate the efficacy of pembrolizumab in patients with advanced sarcomas, characterized by the presence of this potential biomarker [93]. We included 35 patients with TLS-positive advanced STS in this study. The 6-month non-progression rate and ORRs were 40% (95% CI: 22.7%–59.4%) and 30% (95% CI: 14.7%–49.4%), respectively, compared with 4.9% (range: 0.6%–16.5%) and 2.4% (95% CI: 0.1%–12.9%), respectively, in previous cohorts of the PEMBROSARC study, which included all comers [86]. Interestingly, a retrospective analysis of the tumor samples from the patients included in the all-comer cohort displayed that all except one patient harbored a TLS-negative sarcoma, thus suggesting that patient selection based on the presence of TLSs would be an efficient approach toward the identification of an appropriate population for sarcoma-targeted immunotherapy [93].

TABLE 3 Clinical trials investigating immunotherapy in patients with soft-tissue sarcoma

Trial	Design	Treatment	Population / Histotypes			Overall Response Rate			Median progression-free survival					
			Biomarker	Overall	LMS	LPS	UPS	Synovial sarcoma	ASPS	Overall	LMS	LPS	UPS	
Immune checkpoint inhibitors														
SARC028	Initial cohort (Tawbi et al., 2017)	Multi-arm, non-randomized, Phase 2 trial	Pembrolizumab 200mg flat dose q3w	Four cohorts of 10 patients in each histotype: LMS, DDLPS, UPS, synovial sarcoma	17.5%	0%	20%	40%	0%	—	15w	25w	30w	7w
	Expansion cohorts (Burgess, ASCO 2019)		Pembrolizumab 200mg flat dose q3w	Two cohorts: 39 DDLPS and 40 UPS	—	—	10%	23%	—	—	—	2M	3M	—
Alliance A091401	Initial cohort (D'Angelo et al., 2018)	Multi-arm, non-randomized, Phase 2 trial	Nivolumab 3mg/kg q2w	—	5%	—	—	—	—	1.7M	—	—	—	—
	Expansion cohorts (Chen et al., 2020)		Nivolumab 3mg/kg 41 STS + ipilimumab 1mg/kg q3w for 4 cycles followed by nivolumab 3mg/kg q2w	—	16%	—	—	—	—	4.1M	—	—	—	—
Somaiaha, ASCO 2020	Non-randomized, Phase 2 trial	1500mg + tremelimumab 75mg q4w for 4 cycles followed by durvalumab alone	Durvalumab 3mg/kg q2w	14 DDLPS & 14 UPS	—	—	6.7%	7.7%	—	—	—	4.6M	1.5M	—
					—	—	14.3%	28.6%	—	—	—	5.5M	2.7M	34.23M

(Continues)

TABLE 3 (Continued)

Trial			Population / Histotypes		Overall Response Rate		Median progression-free survival				
	Design	Treatment	Biomarker	Overall	LMS	LPS	UPS	Synovial sarcoma	ASPS	Synovial sarcoma	ASPS
D'Angelo, Nature Commun 2022	Non-randomized, Phase 2 trial	Bempegadlesleukin 77 sarcomas (CD122 agonist) 6μg/kg + nivolumab 360mg q3w	-	11.7%	10%	0%	20%	-	25%	-	1.8M 3.9M 2.4M - 2.6M
Immune checkpoint inhibitors + chemotherapy											
PembroSarc Toulmonde, JAMA Oncol 2018	Multi-arm, non-randomized, Phase 2 trial	Cyclophosphamide 41STS 50mg twice daily 1 week on/1 week off + Pembrolizumab 200mg q3w	All-comers	2.4%	0%	-	0%	-	-	1.4M - 1.4M -	
Italiano, Nature Med 2022		30STS TLS positive tumors	-	-	-	-	-	-	4.1M -	-	
Pollack, JAMA Oncol 2020	Non-randomized, Phase 2 trial	Doxorubicin (45mg/m ² and 75mg/m ²) + pembrolizumab 200mg q3w	37STS	-	19%	0%	-	-	8.1M -	-	
Livingston, CCR 2021	Non-randomized, Phase 1/2 trial	Doxorubicin (60mg/m ² with escalation to 75mg/m ²) + pembrolizumab 200mg q3w	30STS	-	36.7%	40%	28.6%	100%	-	5.7M -	
SAINT Gordon, ASCO 2022	Non-randomized, Phase 2 trial	Trabectedin (1.2mg/m ²) q3w + nivolumab 3mg/kg q3w + ipilimumab 1mg/kg q12w	88STS	-	21.6%	-	-	-	-	7M -	
TRAMUNE Toulmonde, Clin Cancer Res 2022	Non-randomized, Phase 1b trial	Trabectedin (1.2mg/m ²) + durvalumab 1120mg q3w	16STS	-	7%	-	-	-	<3M -	-	
Nathenson, ASCO 2020 George, CTOS 2021	Non-randomized, Phase 2 trial	Eribulin (1.4mg/m ²) 20 LPS, 19 LMS, 18 UPS/other sarcomas 200mg q3w	-	17.5%	5.3%	15%	-	-	-	2.5M 6.2M -	

(Continues)

TABLE 3 (Continued)

Trial	Population / Histotypes				Overall Response Rate				Median progression-free survival						
	Design	Treatment	Biomarker	Overall	LMS	LPS	UPS	Synovial sarcoma	ASPS	Overall	LMS	LPS	UPS	Synovial sarcoma	ASPS
Rosenbaum, ASCO 2022	Non-randomized, Phase 1/2 trial	Gemcitabine (900mg/m ² D1, D8) + Docetaxel (75mg/m ² D8)	13 STS with 6 LMS –	33.3%	–	–	–	–	–	>5.5M	–	–	–	–	–
GALLANT Adnan, ASCO 2022	Non-randomized, Phase 2 trial	Gemcitabine (anti-PD-1, 210mg or 375mg D1) q3w	43 STS (600mg/m ² D1, D8), doxorubicin (18mg/m ² D1, D8), docetaxel (25mg/m ² D1, D8) + nivolumab 240mg q2w	18.6%	–	–	–	–	–	>4.6M	–	–	–	–	–
Immune checkpoint inhibitors + antiangiogenics															
Wilky, Lancet Oncol 2020	Non-randomized, Phase 2 trial	Axitinib 5mg twice daily + pembrolizumab 200mg q3w	33 STS with 12 ASPS	–	25%	–	–	–	–	54.5% 4.7M	–	–	–	–	–
Martin-Brito, IMMUNOSAR RTTC 2020	Non-randomized, Phase 1b/2 trial	Sunitinib 37.5mg daily for 2 weeks followed by 25mg daily + nivolumab 3mg/kg q2w	60 STS	–	21.7%	–	–	–	–	5.6M	–	–	–	–	–
Immune checkpoint inhibitors + Oncolytic viruses															
TNT Chawla, ASCO 2021	Non-randomized, Phase 2 trial	Nivolumab (3mg/kg 36 STS q2w) + trabectedin (1.2mg/m ² q3w) + TVEC (intratumoral q2w)	Nivolumab (3mg/kg 36 STS q2w) + trabectedin (1.2mg/m ² q3w) + TVEC (intratumoral q2w)	–	8.3%	–	–	–	–	5.5M	–	–	–	–	–

TABLE 3 (Continued)

Trial	Population / Histotypes			Overall Response Rate			Median progression-free survival								
	Design	Treatment	Biomarker	Overall	LMS	LPS	UPS	Synovial sarcoma	ASPS	Overall	LMS	LPS	UPS	Synovial sarcoma	ASPS
Kelly, JAMA Oncol 2020	Non-randomized, Phase 2 trial	Pembrolizumab (200mg) + TVEC (intratumoral) q3w	20 STS Phase 2 trial	35%	—	—	—	—	—	3.9M	—	—	—	—	—
Immune checkpoint inhibitors in specific histotypes															
Maki, Sarcoma 2013	Non-randomized, Phase 2 trial	Ipilimumab 3mg/kg q3w	6 synovial sarcomas	—	—	—	—	0%	—	—	—	—	—	—	1.85 months
Ben-Ami, Cancer 2017	Non-randomized, Phase 2 trial	Nivolumab 3mg/kg q2w	12 uterine LMS	—	0%	—	—	—	—	—	—	—	—	—	—
Acsé Pem-brolizumab Blay, ASCO 2021	Non-randomized, Phase 2 trial	Pembrolizumab 200mg q3w	Rare sarcomas (incidence<0.2/100,000): 34 chordomas, 14 ASPS, 8 DSRCT, 11 SMARCA4-malignant rhabdoid tumors & 31 others	15.3%	—	—	—	—	50%	2.75 months	—	—	—	—	7.5 months
OSCAR CTOS 2020	Non-randomized, Phase 2 trial	Nivolumab 240mg q2w	11 clear cell sarcomas and 14 ASPS	4%	—	—	—	—	—	7.1% month^a	—	—	—	—	6 months
Gxphore-005 Shi, Clin Cancer Res 2020	Non-randomized, Phase 2 trial	Geptanolimab (anti-PD-1, 3mg/kg q2w)	37 ASPS	—	—	—	—	—	37.8%	—	—	—	—	—	6.9 months

Abbreviations: LMS, leiomyosarcoma; LPS, liposarcoma; UPS, undifferentiated pleomorphic sarcoma; ASPS, alveolar soft part sarcoma; DDSLPS, dedifferentiated liposarcoma; STS, soft tissue sarcoma; M, months; ASCO, American Society of Clinical Oncology

TLSs are observed in approximately 20% of the patients with STS and can be identified in almost all histological subtypes, despite the high proportion of TLS-positive cases in some subtypes (e.g., de-differentiated liposarcoma versus leiomyosarcoma) [92]. The TLS status can be assessed by real-life samples, including small biopsies. Larger samples are more sensitive to detect TLS, which predominate at the tumor front; however, the biopsy samples can be efficiently used to screen TLSs [94]. We recommend a double CD20/CD23 staining to detect TLSs, which offers the advantage of simultaneously ensuring the presence of TLSs comprising B cells (CD20+) and the co-localization of follicular dendritic cells (CD23+).

The identification of a subgroup of sarcoma characterized by the presence of intratumoral TLSs represents an important step towards the development of immunotherapy for patients with sarcoma; nonetheless, researchers are yet to address at least two major questions before emphasizing immunotherapy as a novel and efficient standard of care in patients with STS as follows: how to improve the response rate of TLS-positive sarcomas and how to make immunotherapy an efficient approach in TLS-negative sarcomas?

4.2 | Improving the response rates to ICIs in TLS-positive sarcomas

Simultaneously targeting different immune checkpoints is a potential approach to improve immunotherapy efficacy in patients with TLS+ sarcomas. TLS+ sarcomas are characterized by the increased expression of immune checkpoints besides PD-1, such as cytotoxic T-lymphocyte antigen 4 (CTLA-4), TIGIT or lymphocyte activation gene 3 (LAG3) [91]. LAG3 (CD223) is the third immune checkpoint recently targeted in clinical practice and has garnered considerable interest and scrutiny [95]. LAG3 upregulation is required to control the overt activation and prevent the onset of autoimmunity. However, persistent antigen exposure in the tumor microenvironment (TME) results in sustained LAG3 expression, thus contributing to a state of exhaustion that manifests as impaired proliferation and cytokine production. The exact signaling mechanisms downstream of LAG3 and their interplay with other immune responses remain largely unknown. However, the synergy between LAG3 and PD-1 in multiple settings, coupled with the contrasting intracellular cytoplasmic domain of LAG3, compared with the other immune responses, highlights the potential uniqueness of LAG3. Our research findings [91] and others [96] have demonstrated the strong upregulation of LAG3 in inflamed sarcomas. LAG3+ tumor-infiltrating lymphocytes (TILs) were observed in approximately two-thirds of complex

genomic sarcomas, and their expression was strongly correlated with disease outcomes [96]. Based on this rationale, a clinical trial is currently investigating the activity and safety of nivolumab combined with relatlimab, a monoclonal antibody that targets LAG3, versus nivolumab alone, in patients with STS (<https://www.clinicaltrials.gov/ct2/show/NCT04095208>).

4.3 | Successful immunotherapy in 80% of the patients with TLS-negative sarcoma

Investigating combination strategies with ICIs to transform “cold tumors” into “hot tumors” and improve their sensitivity to ICIs is key to addressing this issue. Several clinical trials are currently investigating the combinations of ICIs with different classes of agents, namely chemotherapy, radiotherapy, toll-like receptor agonists, anti-angiogenics, oncolytic viruses, and epigenetics, that enable the conversion of “cold tumors” to “inflamed tumors”. To better understand the impact of such combinations on the TME, investigators and patients should realize the importance of sequential blood and tissue sampling or a randomized design to avoid any bias in data interpretation. A recent study investigated the combination of doxorubicin and pembrolizumab in patients with advanced STS [97]. The RR (13%) and PFS observed in this phase II study were similar to those observed when doxorubicin was used as a single agent [97]. Unfortunately, the lack of sequential tumor biopsies and randomization precludes any conclusion about the impact of the TME combination and correlations with the clinical benefits, thereby limiting the value of the study in terms of an improvement of knowledge for the scientific community.

4.4 | Immunotherapy for sarcomas beyond ICIs

Besides ICIs, researchers have investigated other immunotherapy strategies in patients with STS. For this review, we focused on T-cell receptor (TCR) gene-modified cells, which are more advanced in terms of clinical development. This therapeutic approach is based on the *ex vivo* expansion of autologous T cells following their genetic engineering to express a novel TCR that recognizes specific tumor antigens. Ongoing clinical trials investigating such TCR-based therapies in patients with STS use TCRs directed at validated cancer germline antigens, i.e., MAGE-A4 and NY-ESO-1, expressed in particular STS subtypes, including myxoid/round cell liposarcoma (MRCLS) and synovial sarcomas.

Ramachandran et al. [98] reported that the adoptive transfer of NY-ESO-1c259 T cells in 42 patients with synovial sarcoma (NCT01343043) was associated with an ORR of 35.7% (15 patients; 1 CR and 14 PR cases) by RECIST. D'Angelo et al. [99] demonstrated that the persistence and functionality of these adoptively transferred T cells were associated with sustained responses in a significant proportion of patients. Moreover, treatment with an autologous T-cell therapy targeting NY-ESO-1 displayed antitumor activity up to 40% ORR and long median PFS, with an acceptable safety profile in a study that enrolled 23 patients with advanced and metastatic MRCLS [100]. Similarly, preliminary data suggested that afamitresgene autoleucel, a genetically modified autologous melanoma-associated antigen 4 (MAGE A4) specific T cell therapy, could induce a prolonged response in heavily pre-treated patients with advanced MAGE-A4-expressing SS and MRCLS [101].

Despite promising preliminary results, the development of TCR-based adoptive cell therapies for treating patients with STS is associated with several challenges, including those associated with manufacturing and processing of the final TCR product, patient selection, optimizing lymphodepletion conditioning, and managing adverse events. Ongoing and future studies will determine the role of TCR therapy in patients with STS.

5 | IMPLEMENTING RADIOMICS TO PREDICT THE BENEFITS OF IMMUNOTHERAPY IN PATIENTS WITH STS

The development of immunotherapy for sarcomas is not an aspect of histology (except for alveolar soft-part sarcoma) but rather that of the TME. Future studies investigating immunotherapy strategies in sarcomas should incorporate at least the presence of TLS as a stratification factor in their design, besides including a strong translational program that will allow for a better understanding of the determinants involved in sensitivity and treatment resistance. Moreover, investigators should explore innovative methods to evaluate the clinical benefits associated with a particular treatment. To date, no STS-specific imaging biomarker has been validated to predict the sensitivity of STS to ICIs and the risk of immunotherapy-related adverse events and to improve the early response evaluation during treatment with ICIs. More than 50 studies have investigated the association between imaging and immune phenotypes or responses to ICIs in solid tumors [102]. Immune-inflamed tumors demonstrate distinct TMEs with dense CD8+ TILs (stimulated by the accumulation of tumor mutation burden and neoantigens) and a high expression of PD-L1; therefore, it should be translated

to conventional imaging, radiomics, and molecular imaging [103]. Solid tumors with a higher proportion of TILs appear to be better circumscribed, with a rounder shape, larger size, various apparent diffusion coefficient values depending on the cancer histology, increased heterogeneity and irregularity on CT scans, and higher homogeneous contrast enhancement on MRI [104, 105]. An exploratory study by Toulmonde et al. [106] specifically involving STS identified a radiomics signature combining nine RFs that distinguished immune-high and -low undifferentiated pleomorphic sarcomas in a small hypothesis-generating cohort of 14 patients (accuracy = 93%). Figure 2 depicts an example of the radiomics application to distinguish immune-high and immune-low STSs.

Multicentric retrospective cohorts have demonstrated the correlations between the radiomics patterns on CE-CT scans and response to ICIs, including multiple solid tumors (AUC = 0.83 for predicting ICI response in a non-small cell lung cancer cohort in the study by Trebeschi et al. [105] and multivariate hazard ratio for high radiomics score group = 0.52 [0.34–0.79] in the study by Sun et al. [107]). Researchers should investigate the validation and adaptation of these radiomics scores for patients with STS treated with ICIs.

The early prediction of the response to an ICI may be enhanced using radiomics and molecular imaging. RECIST has been replaced by immune-RECIST to reduce the confusion between true progression and pseudo-progression. Likewise, the PET response criteria for solid tumors (PERCIST) have been replaced by immune-PERCIST and PET response evaluation criteria for immunotherapy [108–110]. However, researchers have evaluated neither their added value in terms of predicting the OS or PFS in patients with STS undergoing ICI therapy nor that of delta-radiomics approaches.

Eventually, ¹⁸F-FDG has proven to lack the specificity and consistency for robustly discriminating TMEs associated with distinct outcomes under ICI treatment; therefore, investigators are designing novel tracers with monoclonal antibodies (or antibody fragments) targeting PD-1 (such as Zirconium-89-nivolumab), PD-L1 (such as ¹⁸F-BMS-986192 adnectin), CTLA-4 (such as Zirconium-89-ipilimumab), CD8+ lymphocytes (such as Zirconium-89-Df-IAB22M2C), or interleukin-2 receptor (such as Technetium-99-IL2), under the name of immuno-PET [111–113]. Beyond preclinical patient-derived xenograft studies, ongoing clinical trials have been evaluating the tolerance, distribution, and interest of these tracers in patients with non-small cell lung cancer, thus revealing correlations with tumors expressing PD-L1 ≥50% on IHCs, high numbers of TILs, and the response to anti-PD-1 immunotherapy [114–116]. However, none of these methods have been attempted in patients with STS or STS xenografts.

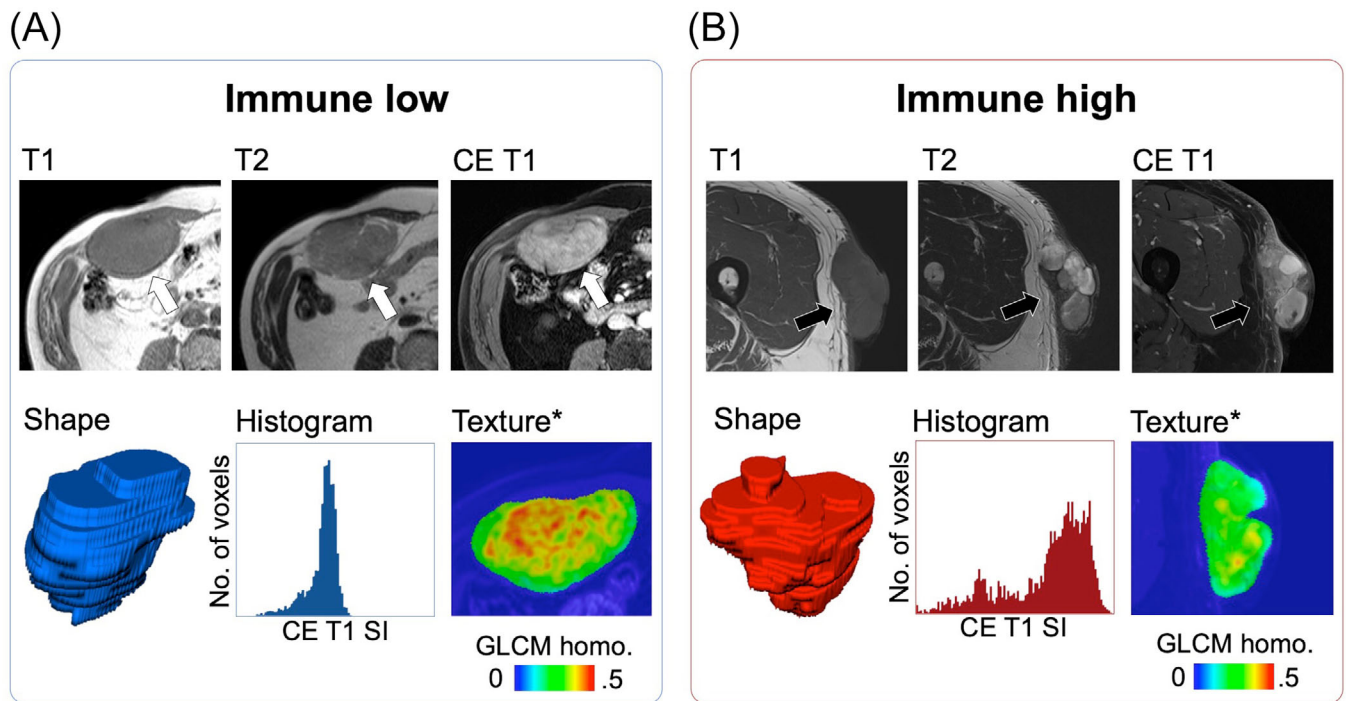


FIGURE 2 Radiomics to distinguish between immune low (A) and high UPS (B) according to Toulmonde et al. [106]. On contrast-enhanced MRI, immune high UPS (black arrows) is characterized by a more heterogeneous aspect than immune low UPS (white arrows), captured through a combination of nine radiomics features, all related to heterogeneity. *The local texture map corresponds to the GLCM homogeneity (homo.) calculated on a small tile (or kernel) of 3×3 voxels. Higher values correspond to greater local homogeneity. Abbreviations: CE: contrast-enhanced; MRI: magnetic resonance imaging; No.: number; SI: signal intensity; UPS: undifferentiated pleomorphic sarcomas; GLCM: gray-level co-occurrence matrix. This figure is original.

6 | CONCLUSIONS

In conclusion, innovative diagnostic technologies, such as digital pathology, and quantitative multimodal multiparametric imaging, including radiomics, can enhance the diagnosis, prognosis assessment, and treatment monitoring of STS. Further studies are required to evaluate the impact of their implementation in routine practice. Recent research has revealed the potential for efficient immunotherapies against sarcoma. While capturing the heterogeneity of STS is challenging, ICI-based regimens are likely the strategy for patients with TLS-positive tumors. Clinicians should implement innovative approaches based on a stringent characterization of the STS microenvironment in patients with TLS-negative tumors.

AUTHOR CONTRIBUTIONS

Concept and design: AI; drafting of the manuscript: AC and AI; and supervision: AI. All authors participated in writing and revising this work.

ACKNOWLEDGMENTS

None.

CONFLICT OF INTEREST STATEMENT

AI: Research grant: AstraZeneca, Bayer, BMS Merck, MSD, and Roche. Advisory Board: AstraZeneca, Bayer, Janssen Cilag, Lilly, Roche, Blueprint medicines, and PharmaMar. AC: No competing interests.

FUNDING

Agence Nationale de la Recherche (RHU CONDOR).

DATA AVAILABILITY STATEMENT

Not applicable.

ETHICS APPROVAL AND CONSENT TO PARTICIPATE

Not applicable.

CONSENT FOR PUBLICATION

Not applicable.

ORCIDAntoine Italiano <https://orcid.org/0000-0002-8540-5351>**REFERENCES**

1. Italiano A, Mathoulin-Pelissier S, Cesne AL, Terrier P, Bonvalot S, Collin F, et al. Trends in survival for patients with metastatic soft-tissue sarcoma. *Cancer*. 2011;117(5):1049-1054.
2. Callegaro D, Miceli R, Bonvalot S, Ferguson PC, Strauss DC, van Praag VVM, et al. development and external validation of a dynamic prognostic nomogram for primary extremity soft tissue sarcoma survivors. *EClinicalMedicine*. 2019;17:100215.
3. Pervaiz N, Colterjohn N, Farrokhyar F, Tozer R, Figueiredo A, Ghert M. A systematic meta-analysis of randomized controlled trials of adjuvant chemotherapy for localized resectable soft-tissue sarcoma. *Cancer*. 2008;113(3):573-581.
4. Issels RD, Lindner LH, Verweij J, Wust P, Reichardt P, Schem B-C, et al. Neo-adjuvant chemotherapy alone or with regional hyperthermia for localised high-risk soft-tissue sarcoma: a randomised phase 3 multicentre study. *Lancet Oncol*. 2010;11(6):561-570.
5. Italiano A, Le Cesne A, Mendiboure J, Blay J-Y, Piperno-Neumann S, Chevreau C, et al. Prognostic factors and impact of adjuvant treatments on local and metastatic relapse of soft-tissue sarcoma patients in the competing risks setting. *Cancer*. 2014;120(21):3361-3369.
6. Gronchi A, Ferrari S, Quagliuolo V, Broto JM, Pousa AL, Grignani G, et al. Histotype-tailored neoadjuvant chemotherapy versus standard chemotherapy in patients with high-risk soft-tissue sarcomas (ISG-STS 1001): an international, open-label, randomised, controlled, phase 3, multicentre trial. *Lancet Oncol*. 2017;18(6):812-822.
7. Italiano A, Stoeckle E. Role of perioperative chemotherapy in soft-tissue sarcomas: It's time to end a never-ending story. *Eur J Cancer*. 2018;97:53-54.
8. Rothermundt C, Fischer GF, Bauer S, Blay J-Y, Grünwald V, Italiano A, et al. Pre- and Postoperative Chemotherapy in Localized Extremity Soft Tissue Sarcoma: A European Organization for Research and Treatment of Cancer Expert Survey. *Oncologist*. 2018;23(4):461-467.
9. Callegaro D, Miceli R, Bonvalot S, Ferguson P, Strauss DC, Levy A, et al. development and external validation of two nomograms to predict overall survival and occurrence of distant metastases in adults after surgical resection of localised soft-tissue sarcomas of the extremities: a retrospective analysis. *The Lancet Oncology*. 2016;17(5):671-680.
10. Crombé A, Spalato-Ceruso M, Michot A, Laizet Y, Lucchesi C, Toulmonde M, et al. Gene expression profiling improves prognostication by nomogram in patients with soft-tissue sarcomas. *Cancer Commun (Lond)*. 2022;42(6):563-566.
11. Huang S, Yang J, Fong S, Zhao Q. Artificial intelligence in cancer diagnosis and prognosis: Opportunities and challenges. *Cancer Lett*. 2020;471:61-71.
12. Courtiol P, Maussion C, Moarii M, Pronier E, Pilcer S, Sefta M, et al. Deep learning-based classification of mesothelioma improves prediction of patient outcome. *Nat Med*. 2019;25(10):1519-1525.
13. Saillard C, Schmauch B, Laifa O, Moarii M, Toldo S, Zaslavskiy M, et al. Predicting Survival After Hepatocellular Carcinoma Resection Using Deep Learning on Histological Slides. *Hepatology*. 2020;72(6):2000-2013.
14. Boehm KM, Khosravi P, Vanguri R, Gao J, Shah SP. Harnessing multimodal data integration to advance precision oncology. *Nat Rev Cancer*. 2022;22(2):114-126.
15. Foersch S, Eckstein M, Wagner D-C, Gach F, Woerl A-C, Geiger J, et al. Deep learning for diagnosis and survival prediction in soft tissue sarcoma. *Ann Oncol*. 2021;32(9):1178-1187.
16. Gronchi A, Miah AB, Dei Tos AP, Abecassis N, Bajpai J, Bauer S, et al. Soft tissue and visceral sarcomas: ESMO-EURACAN-GENTURIS Clinical Practice Guidelines for diagnosis, treatment and follow-up. *Ann Oncol*. 2021;32(11):1348-1365.
17. Eisenhauer EA, Therasse P, Bogaerts J, Schwartz LH, Sargent D, Ford R, et al. New response evaluation criteria in solid tumours: revised RECIST guideline (version 1.1). *Eur J Cancer*. 2009;45(2):228-247.
18. Gillies RJ, Kinahan PE, Hricak H. Radiomics: Images Are More than Pictures, They Are Data. *Radiology*. 2016;278(2):563-577.
19. Abousaway O, Rakhsandehroo T, Van den Abbeele AD, Kircher MF, Rashidian M. Noninvasive Imaging of Cancer Immunotherapy. *Nanotheranostics*. 2021;5(1):90-112.
20. Lambin P, Leijenaar RTH, Deist TM, Peerlings J, de Jong EEC, van Timmeren J, et al. Radiomics: the bridge between medical imaging and personalized medicine. *Nat Rev Clin Oncol*. 2017;14(12):749-762.
21. Crombé A, Matcuk GR, Fadli D, Sambri A, Patel DB, Paioli A, et al. Role of Imaging in Initial Prognostication of Locally Advanced Soft Tissue Sarcomas. *Acad Radiol*. 2022;S1076-6332(22)00250-1 (online ahead of print).
22. Spinnato P, Kind M, Le Loarer F, Bianchi G, Colangeli M, Sambri A, et al. Soft Tissue Sarcomas: The Role of Quantitative MRI in Treatment Response Evaluation. *Acad Radiol*. 2021;S1076-6332(21)00360-3.
23. Limkin EJ, Sun R, Dercle L, Zacharakis EI, Robert C, Reuzé S, et al. Promises and challenges for the implementation of computational medical imaging (radiomics) in oncology. *Ann Oncol*. 2017;28(6):1191-1206.
24. Steyerberg EW, Vickers AJ, Cook NR, Gerds T, Gonen M, Obuchowski N, et al. Assessing the performance of prediction models: a framework for some traditional and novel measures. *Epidemiology*. 2010;21(1):128-138.
25. Vickers AJ, Elkin EB. Decision curve analysis: a novel method for evaluating prediction models. *Med Decis Making*. 2006;26(6):565-574.
26. Chollet F. Xception: Deep Learning with Depthwise Separable Convolutions. 2017. F.Chollet, Xception: Deep Learning with Depthwise Separable Convolutions. *IEEE Conference on Computer Vision and Pattern Recognition (CVPR)*. 2017;1800-1807.
27. Simonyan K, Zisserman A. Very Deep Convolutional Networks for Large-Scale Image Recognition. 2015. Available from: <https://arXiv.org/abs/1409.1556>
28. He K, Zhang X, Ren S, Sun J. Deep Residual Learning for Image Recognition. *IEEE Conference on Computer Vision and Pattern Recognition (CVPR)*. 2016;770-778.
29. Szegedy C, Vanhoucke V, Ioffe S, Shlens J, Wojna, Z. Rethinking the Inception Architecture for Computer Vision. *IEEE Conference on Computer Vision and Pattern Recognition (CVPR)*. 2016;2818-2826

30. Russakovsky O, Deng J, Su H, Krause J, Satheesh S, et al. ImageNet Large Scale Visual Recognition Challenge. *Int J Comput Vis* 2015;115:211-252.
31. Navarro F, Dapper H, Asadpour R, Knebel C, Spraker MB, Schwarze V, et al. Development and External Validation of Deep-Learning-Based Tumor Grading Models in Soft-Tissue Sarcoma Patients Using MR Imaging. *Cancers (Basel)*. 2021;13(12):2866.
32. Yue Z, Wang X, Yu T, Shang S, Liu G, Jing W, et al. Multi-parametric MRI-based radiomics for the diagnosis of malignant soft-tissue tumor. *Magn Reson Imaging*. 2022;91:91-99.
33. Peeken JC, Spraker MB, Knebel C, Dapper H, Pfeiffer D, Devecka M, et al. Tumor grading of soft tissue sarcomas using MRI-based radiomics. *EBioMedicine*. 2019;48:332-340.
34. Yan R, Hao D, Li J, Liu J, Hou F, Chen H, et al. Magnetic Resonance Imaging-Based Radiomics Nomogram for Prediction of the Histopathological Grade of Soft Tissue Sarcomas: A Two-Center Study. *J Magn Reson Imaging*. 2021;53(6):1683-1696.
35. Yang Y, Zhou Y, Zhou C, Zhang X, Ma X. MRI-Based Computer-Aided Diagnostic Model to Predict Tumor Grading and Clinical Outcomes in Patients With Soft Tissue Sarcoma. *J Magn Reson Imaging*. 2022 (online ahead of print).
36. Chen S, Li N, Tang Y, Chen B, Fang H, Qi S, et al. Radiomics Analysis of Fat-Saturated T2-Weighted MRI Sequences for the Prediction of Prognosis in Soft Tissue Sarcoma of the Extremities and Trunk Treated With Neoadjuvant Radiotherapy. *Front Oncol*. 2021;11:710649.
37. Liu S, Sun W, Yang S, Duan L, Huang C, Xu J, et al. Deep learning radiomic nomogram to predict recurrence in soft tissue sarcoma: a multi-institutional study. *Eur Radiol*. 2022;32(2):793-805.
38. Gillies RJ, Anderson AR, Gatenby RA, Morse DL. The biology underlying molecular imaging in oncology: from genome to anatome and back again. *Clin Radiol*. 2010;65(7):517-521.
39. Junut J, Sijbers J, De Backer S, Rajan J, Van Dyck D. Machine learning study of several classifiers trained with texture analysis features to differentiate benign from malignant soft-tissue tumors in T1-MRI images. *J Magn Reson Imaging*. 2010;31(3):680-689.
40. Martin-Carreras T, Li H, Cooper K, Fan Y, Sebro R. Radiomic features from MRI distinguish myxomas from myxofibrosarcomas. *BMC Med Imaging*. 2019;19(1):67.
41. Fields BKK, Demirjian NL, Hwang DH, Varghese BA, Cen SY, Lei X, et al. Whole-tumor 3D volumetric MRI-based radiomics approach for distinguishing between benign and malignant soft tissue tumors. *Eur Radiol*. 2021;31(11):8522-8535.
42. Lee SE, Jung J-Y, Nam Y, Lee S-Y, Park H, Shin S-H, et al. Radiomics of diffusion-weighted MRI compared to conventional measurement of apparent diffusion-coefficient for differentiation between benign and malignant soft tissue tumors. *Sci Rep*. 2021;11(1):15276.
43. Thornhill RE, Golfam M, Sheikh A, Cron GO, White EA, Werier J, et al. Differentiation of lipoma from liposarcoma on MRI using texture and shape analysis. *Acad Radiol*. 2014;21(9):1185-1194.
44. Vos M, Starmans MPA, Timmergen MJM, van der Voort SR, Padmos GA, Kessels W, et al. Radiomics approach to distinguish between well differentiated liposarcomas and lipomas on MRI. *Br J Surg*. 2019;106(13):1800-1809.
45. Pressney I, Khoo M, Endozo R, Ganeshan B, O'Donnell P. Pilot study to differentiate lipoma from atypical lipomatous tumour/well-differentiated liposarcoma using MR radiomics-based texture analysis. *Skeletal Radiol*. 2020;49(11):1719-1729.
46. Malinauskaitė I, Hofmeister J, Burgermeister S, Neroladaki A, Hamard M, Montet X, et al. Radiomics and Machine Learning Differentiate Soft-Tissue Lipoma and Liposarcoma Better than Musculoskeletal Radiologists. *Sarcoma*. 2020;2020:7163453.
47. Leporq B, Bouhamama A, Pilleul F, Lame F, Bihane C, Sdika M, et al. MRI-based radiomics to predict lipomatous soft tissue tumors malignancy: a pilot study. *Cancer Imaging*. 2020;20(1):78.
48. Yang Y, Zhou Y, Zhou C, Ma X. Novel computer aided diagnostic models on multimodality medical images to differentiate well differentiated liposarcomas from lipomas approached by deep learning methods. *Orphanet J Rare Dis*. 2022;17(1):158.
49. Gerges L, Popolek D, Rosenkrantz AB. Explorative Investigation of Whole-Lesion Histogram MRI Metrics for Differentiating Uterine Leiomyomas and Leiomyosarcomas. *American Journal of Roentgenology*. 2018;210(5):1172-1177.
50. Nakagawa M, Nakaura T, Namimoto T, Iyama Y, Kidoh M, Hirata K, et al. Machine Learning to Differentiate T2-Weighted Hyperintense Uterine Leiomyomas from Uterine Sarcomas by Utilizing Multiparametric Magnetic Resonance Quantitative Imaging Features. *Academic Radiology*. 2019;26(10):1390-1399.
51. Xie H, Hu J, Zhang X, Ma S, Liu Y, Wang X. Preliminary utilization of radiomics in differentiating uterine sarcoma from atypical leiomyoma: Comparison on diagnostic efficacy of MRI features and radiomic features. *Eur J Radiol*. 2019;115:39-45. <https://doi.org/10.1016/j.ejrad.2019.04.004>
52. Wang T, Gong J, Li Q, Chu C, Shen W, Peng W, et al. A combined radiomics and clinical variables model for prediction of malignancy in T2 hyperintense uterine mesenchymal tumors on MRI. *Eur Radiol*. 2021;31(8):6125-6135.
53. Dai M, Liu Y, Hu Y, Li G, Zhang J, Xiao Z, et al. Combining multi-parametric MRI features-based transfer learning and clinical parameters: application of machine learning for the differentiation of uterine sarcomas from atypical leiomyomas. *Eur Radiol*. 2022.
54. Corino VDA, Montin E, Messina A, Casali PG, Gronchi A, Marchianò A, et al. Radiomic analysis of soft tissues sarcomas can distinguish intermediate from high-grade lesions. *J Magn Reson Imaging*. 2018;47(3):829-840.
55. Zhang Y, Zhu Y, Shi X, Tao J, Cui J, Dai Y, et al. Soft Tissue Sarcomas: Preoperative Predictive Histopathological Grading Based on Radiomics of MRI. *Acad Radiol*. 2019;26(9):1262-1268.
56. Crombé A, Marcellin P-J, Buy X, Stoeckle E, Brouste V, Italiano A, et al. Soft-Tissue Sarcomas: Assessment of MRI Features Correlating with Histologic Grade and Patient Outcome. *Radiology*. 2019;291(3):710-721.
57. Schneider N, Strauss DC, Smith MJ, Miah AB, Zaidi S, Benson C, et al. The Adequacy of Core Biopsy in the Assessment of Smooth Muscle Neoplasms of Soft Tissues: Implications for Treatment and Prognosis. *Am J Surg Pathol*. 2017;41(7):923-931.
58. Vallières M, Freeman CR, Skamene SR, El Naqa I. A radiomics model from joint FDG-PET and MRI texture features for the prediction of lung metastases in soft-tissue sarcomas of the extremities. *Phys Med Biol*. 2015;60(14):5471-5496.

59. Peeken JC, Bernhofer M, Spraker MB, Pfeiffer D, Devecka M, Thamer A, et al. CT-based radiomic features predict tumor grading and have prognostic value in patients with soft tissue sarcomas treated with neoadjuvant radiation therapy. *Radither Oncol.* 2019;135:187-196.
60. Crombé A, Kind M, Fadli D, Le Loarer F, Italiano A, Buy X, et al. Intensity harmonization techniques influence radiomics features and radiomics-based predictions in sarcoma patients. *Sci Rep.* 2020;10(1):15496.
61. Crombé A, Le Loarer F, Sitbon M, Italiano A, Stoeckle E, Buy X, et al. Can radiomics improve the prediction of metastatic relapse of myxoid/round cell liposarcomas? *Eur Radiol.* 2020;30(5):2413-2424.
62. Yang Y, Ma X, Wang Y, Ding X. Prognosis prediction of extremity and trunk wall soft-tissue sarcomas treated with surgical resection with radiomic analysis based on random survival forest. *Updates Surg.* 2022;74(1):355-365.
63. Peeken JC, Neumann J, Asadpour R, Leonhardt Y, Moreira JR, Hippel DS, et al. Prognostic Assessment in High-Grade Soft-Tissue Sarcoma Patients: A Comparison of Semantic Image Analysis and Radiomics. *Cancers (Basel).* 2021;13(8):1929.
64. Fadli D, Kind M, Michot A, Le Loarer F, Crombé A. Natural Changes in Radiological and Radiomics Features on MRIs of Soft-Tissue Sarcomas Naïve of Treatment: Correlations With Histology and Patients' Outcomes. *J Magn Reson Imaging.* 2022;56(1):77-96.
65. Crombé A, Fadli D, Buy X, Italiano A, Saut O, Kind M. High-Grade Soft-Tissue Sarcomas: Can Optimizing Dynamic Contrast-Enhanced MRI Postprocessing Improve Prognostic Radiomics Models? *J Magn Reson Imaging.* 2020;52(1):282-297.
66. Crombé A, Périer C, Kind M, De Senneville BD, Le Loarer F, Italiano A, et al. T2 -based MRI Delta-radiomics improve response prediction in soft-tissue sarcomas treated by neoadjuvant chemotherapy. *J Magn Reson Imaging.* 2019;50(2):497-510.
67. Crombé A, Saut O, Guigui J, Italiano A, Buy X, Kind M. Influence of temporal parameters of DCE-MRI on the quantification of heterogeneity in tumor vascularization. *J Magn Reson Imaging.* 2019;50(6):1773-1788.
68. Gao Y, Kalbasi A, Hsu W, Ruan D, Fu J, Shao J, et al. Treatment effect prediction for sarcoma patients treated with preoperative radiotherapy using radiomics features from longitudinal diffusion-weighted MRIs. *Phys Med Biol.* 2020;65(17):175006.
69. Peeken JC, Asadpour R, Specht K, Chen EY, Klymenko O, Akinkuoroje V, et al. MRI-based delta-radiomics predicts pathologic complete response in high-grade soft-tissue sarcoma patients treated with neoadjuvant therapy. *Radiother Oncol.* 2021;164:73-82.
70. Chibon F, Lagarde P, Salas S, Péröt G, Brouste V, Tirole F, et al. Validated prediction of clinical outcome in sarcomas and multiple types of cancer on the basis of a gene expression signature related to genome complexity. *Nat Med.* 2010;16(7):781-787.
71. O'Connor JPB, Aboagye EO, Adams JE, Aerts HJWL, Barrington SF, Beer AJ, et al. Imaging biomarker roadmap for cancer studies. *Nat Rev Clin Oncol.* 2017;14(3):169-186.
72. Zwanenburg A, Vallières M, Abdalah MA, Aerts HJWL, Andarczyk V, Apte A, et al. The Image Biomarker Standardization Initiative: Standardized Quantitative Radiomics for High-Throughput Image-based Phenotyping. *Radiology.* 2020;295(2):328-338.
73. Vallières M, Zwanenburg A, Badic B, Cheze Le Rest C, Visvikis D, Hatt M. Responsible Radiomics Research for Faster Clinical Translation. *J Nucl Med.* 2018;59(2):189-193.
74. Clark K, Vendt B, Smith K, Freymann J, Kirby J, Koppel P, et al. The Cancer Imaging Archive (TCIA): Maintaining and Operating a Public Information Repository. *J Digit Imaging.* 2013;26(6):1045-1057.
75. Ronneberger O, Fischer P, Brox T. U-Net: Convolutional Networks for Biomedical Image Segmentation. 1st ed. Springer: Medical Image Computing and Computer-Assisted Intervention – MICCAI 2015. Lecture Notes in Computer Science. 2015;9351:234-241. https://doi.org/10.1007/978-3-319-24574-4_28
76. Benjamin RS, Wiernik PH, Bachur NR. Adriamycin chemotherapy-efficacy, safety, and pharmacologic basis of an intermittent single high-dosage schedule. *Cancer.* 1974;33(1):19-27.
77. Keung EZ, Wargo JA. The Current Landscape of Immune Checkpoint Inhibition for Solid Malignancies. *Surg Oncol Clin N Am.* 2019;28(3):369-386.
78. Jungbluth AA, Antonescu CR, Busam KJ, Iversen K, Kolb D, Coplan K, et al. Monophasic and biphasic synovial sarcomas abundantly express cancer/testis antigen NY-ESO-1 but not MAGE-A1 or CT7. *Int J Cancer.* 2001;94(2):252-256.
79. Pollack SM, Jungbluth AA, Hoch BL, Farrar EA, Bleakley M, Schneider DJ, et al. NY-ESO-1 is a ubiquitous immunotherapeutic target antigen for patients with myxoid/round cell liposarcoma. *Cancer.* 2012;118(18):4564-4570.
80. Hemminger JA, Iwenofu OH. NY-ESO-1 is a sensitive and specific immunohistochemical marker for myxoid and round cell liposarcomas among related mesenchymal myxoid neoplasms. *Mod Pathol.* 2013;26(9):1204-1210.
81. Orui H, Ishikawa A, Okada K, Nishida J, Mitsui H, Kashiwa H, et al. Dendritic cell and effector cell infiltration in soft tissue sarcomas with reactive lymphoid hyperplasia. *J Orthop Sci.* 2003;8(5):669-677.
82. Tseng WW, Demicco EG, Lazar AJ, Lev DC, Pollock RE. Lymphocyte composition and distribution in inflammatory, well-differentiated retroperitoneal liposarcoma: clues to a potential adaptive immune response and therapeutic implications. *Am J Surg Pathol.* 2012;36(6):941-944.
83. Frezza AM, Stacchiotti S, Gronchi A. Highlights in soft tissue sarcomas and gastrointestinal stromal tumours (GIST) trials reported at ASCO 2017 Annual Meeting. *BMC Med.* 2017;15(1):160. <https://doi.org/10.1186/s12916-017-0931-4>
84. D'Angelo SP, Mahoney MR, Van Tine BA, Atkins J, Milhem MM, Jahagirdar BN, et al. Nivolumab with or without ipilimumab treatment for metastatic sarcoma (Alliance A091401): two open-label, non-comparative, randomised, phase 2 trials. *Lancet Oncol.* 2018;19(3):416-426.
85. Tawbi HA, Burgess M, Bolejack V, Van Tine BA, Schuetze SM, Hu J, et al. Pembrolizumab in advanced soft-tissue sarcoma and bone sarcoma (SARC028): a multicentre, two-cohort, single-arm, open-label, phase 2 trial. *Lancet Oncol.* 2017;18(11):1493-1501.
86. Toulmonde M, Penel N, Adam J, Chevreau C, Blay J-Y, Le Cesne A, et al. Use of PD-1 Targeting, Macrophage Infiltration, and IDO Pathway Activation in Sarcomas: A Phase 2 Clinical Trial. *JAMA Oncol.* 2018;4(1):93-97.

87. Italiano A, Bellera C, D'Angelo S. PD1/PD-L1 targeting in advanced soft-tissue sarcomas: a pooled analysis of phase II trials. *J Hematol Oncol.* 2020;13(1):55.
88. Naqash AR, O'Sullivan Coyne GH, Moore N, Sharon E, Takebe N, Fino KK, et al. Phase II study of atezolizumab in advanced alveolar soft part sarcoma (ASPS). *JCO.* 2021;39(15_suppl):11519–11519.
89. Wilky BA, Trucco MM, Subhawong TK, Florou V, Park W, Kwon D, et al. Axitinib plus pembrolizumab in patients with advanced sarcomas including alveolar soft-part sarcoma: a single-centre, single-arm, phase 2 trial. *Lancet Oncol.* 2019;20(6):837–848.
90. Trabucco SE, Ali SM, Sokol E, Schrock AB, Albacker LA, Chung J, et al. Frequency of genomic biomarkers of response to immunotherapy in sarcoma. *JCO.* 2018;36(15_suppl):11579–11579.
91. Petitprez F, de Reyniès A, Keung EZ, Chen TW-W, Sun C-M, Calderaro J, et al. B cells are associated with survival and immunotherapy response in sarcoma. *Nature.* 2020;577(7791):556–560.
92. Sautès-Fridman C, Petitprez F, Calderaro J, Fridman WH. Tertiary lymphoid structures in the era of cancer immunotherapy. *Nat Rev Cancer.* 2019;19(6):307–325.
93. Italiano A, Bessede A, Pulido M, Bompas E, Piperno-Neumann S, Chevreau C, et al. Pembrolizumab in soft-tissue sarcomas with tertiary lymphoid structures: a phase 2 PEMBROSARC trial cohort. *Nat Med.* 2022;28(6):1199–1206.
94. Vanhersecke L, Brunet M, Guégan J-P, Rey C, Bougouin A, Cousin S, et al. Mature tertiary lymphoid structures predict immune checkpoint inhibitor efficacy in solid tumors independently of PD-L1 expression. *Nat Cancer.* 2021;2(8):794–802.
95. Shi A-P, Tang X-Y, Xiong Y-L, Zheng K-F, Liu Y-J, Shi X-G, et al. Immune Checkpoint LAG3 and Its Ligand FGL1 in Cancer. *Front Immunol.* 2021;12:785091.
96. Que Y, Fang Z, Guan Y, Xiao W, Xu B, Zhao J, et al. LAG-3 expression on tumor-infiltrating T cells in soft tissue sarcoma correlates with poor survival. *Cancer Biol Med.* 2019;16(2):331–340.
97. Pollack SM, Redman MW, Baker KK, Wagner MJ, Schroeder BA, Loggers ET, et al. Assessment of Doxorubicin and Pembrolizumab in Patients With Advanced Anthracycline-Naïve Sarcoma: A Phase 1/2 Nonrandomized Clinical Trial. *JAMA Oncol.* 2020;6(11):1778–1782.
98. Ramachandran I, Lowther DE, Dryer-Minnerly R, Wang R, Fayngerts S, Nunez D, et al. Systemic and local immunity following adoptive transfer of NY-ESO-1 SPEAR T cells in synovial sarcoma. *J Immunother Cancer.* 2019;7(1):276.
99. D'Angelo SP, Melchiori L, Merchant MS, Bernstein D, Glod J, Kaplan R, et al. Antitumor Activity Associated with Prolonged Persistence of Adoptively Transferred NY-ESO-1 c259T Cells in Synovial Sarcoma. *Cancer Discov.* 2018;8(8):944–957.
100. D'Angelo SP, Druta M, Van Tine BA, Liebner DA, Schuetze S, Nathenson M, et al. Primary efficacy and safety of letetrastegene autoleucel (lete-cel; GSK3377794) pilot study in patients with advanced and metastatic myxoid/round cell liposarcoma (MRCLS). *JCO.* 2022;40(16_suppl):11500–11500.
101. D'Angelo SP, Van Tine BA, Attia S, Blay J-Y, Strauss SJ, Valverde Morales CM, et al. SPEARHEAD-1: A phase 2 trial of afamitresgene autoleucel (Formerly ADP-A2M4) in patients with advanced synovial sarcoma or myxoid/round cell liposarcoma. *JCO.* 2021;39(15_suppl):11504–11504.
102. Wang JH, Wahid KA, van Dijk LV, Farahani K, Thompson RF, Fuller CD. Radiomic biomarkers of tumor immune biology and immunotherapy response. *Clin Transl Radiat Oncol.* 2021;28:97–115.
103. Hegde PS, Karanikas V, Evers S. The Where, the When, and the How of Immune Monitoring for Cancer Immunotherapies in the Era of Checkpoint Inhibition. *Clin Cancer Res.* 2016;22(8):1865–1874.
104. Çelebi F, Agacayak F, Ozturk A, Ilgun S, Ucuncu M, Iyigun ZE, et al. Usefulness of imaging findings in predicting tumor-infiltrating lymphocytes in patients with breast cancer. *Eur Radiol.* 2020;30(4):2049–2057.
105. Trebeschi S, Drago SG, Birkbak NJ, Kurilova I, Călin AM, Delli Pizzi A, et al. Predicting response to cancer immunotherapy using non-invasive radiomic biomarkers. *Ann Oncol.* 2019;30(6):998–1004.
106. Toulmonde M, Lucchesi C, Verbeke S, Crombe A, Adam J, Geneste D, et al. High throughput profiling of undifferentiated pleomorphic sarcomas identifies two main subgroups with distinct immune profile, clinical outcome and sensitivity to targeted therapies. *EBioMedicine.* 2020;62:103131.
107. Sun R, Limkin EJ, Vakalopoulou M, Dercle L, Champiat S, Han SR, et al. A radiomics approach to assess tumour-infiltrating CD8 cells and response to anti-PD-1 or anti-PD-L1 immunotherapy: an imaging biomarker, retrospective multicohort study. *Lancet Oncol.* 2018;19(9):1180–1191. [https://doi.org/10.1016/S1470-2045\(18\)30413-3](https://doi.org/10.1016/S1470-2045(18)30413-3)
108. Seymour L, Bogaerts J, Perrone A, Ford R, Schwartz LH, Mandrekar S, et al. iRECIST: guidelines for response criteria for use in trials testing immunotherapeutics. *Lancet Oncol.* 2017;18(3):e143–e152.
109. Anwar H, Sachpekidis C, Winkler J, Kopp-Schneider A, Haberkorn U, Hassel JC, et al. Absolute number of new lesions on 18F-FDG PET/CT is more predictive of clinical response than SUV changes in metastatic melanoma patients receiving ipilimumab. *Eur J Nucl Med Mol Imaging.* 2018;45(3):376–383.
110. Goldfarb L, Duchemann B, Chouahnia K, Zelek L, Soussan M. Monitoring anti-PD-1-based immunotherapy in non-small cell lung cancer with FDG PET: introduction of iPERCIST. *EJNMMI Res.* 2019;9(1):8.
111. Borm FJ, Smit J, Oprea-Lager DE, Wondergem M, Haanen JBAG, Smit EF, et al. Response Prediction and Evaluation Using PET in Patients with Solid Tumors Treated with Immunotherapy. *Cancers (Basel).* 2021;13(12):3083.
112. van de Donk PP, Kist de Ruijter L, Lub-de Hooge MN, Brouwers AH, van der Wekken AJ, Oosting SF, et al. Molecular imaging biomarkers for immune checkpoint inhibitor therapy. *Theranostics.* 2020;10(4):1708–1718.
113. Filippi L, Nervi C, Proietti I, Pirisino R, Potenza C, Martelli O, et al. Molecular imaging in immuno-oncology: current status and translational perspectives. *Expert Rev Mol Diagn.* 2020;20(12):1199–1211.
114. Bensch F, van der Veen EL, Lub-de Hooge MN, Jorritsma-Smit A, Boellaard R, Kok IC, et al. 89Zr-atezolizumab imaging as a non-invasive approach to assess clinical response to PD-L1 blockade in cancer. *Nat Med.* 2018;24(12):1852–1858.

115. Niemeijer AN, Leung D, Huisman MC, Bahce I, Hoekstra OS, van Dongen GAMS, et al. Whole body PD-1 and PD-L1 positron emission tomography in patients with non-small-cell lung cancer. *Nat Commun.* 2018;9(1):4664.
116. Huisman MC, Niemeijer A-LN, Windhorst AD, Schuit RC, Leung D, Hayes W, et al. Quantification of PD-L1 Expression with 18F-BMS-986192 PET/CT in Patients with Advanced-Stage Non-Small Cell Lung Cancer. *J Nucl Med.* 2020;61(10):1455-1460.

How to cite this article: Crombé A, Roulleau-Dugage M, Italiano A. The diagnosis, classification, and treatment of sarcoma in this era of artificial intelligence and immunotherapy. *Cancer Communications.* 2022;1-26.
<https://doi.org/10.1002/cac2.12373>